Pixel array detectors for time resolved radiography (invited)

M. J. Renzi,[a] M. W. Tate, A. Ercan, and S. M. Gruner[b]
Department of Physics, Cornell University, Ithaca, New York 14853

E. Fontes
CHESS, Cornell University, Ithaca, New York 14853

C. F. Powell, A. G. MacPhee, S. Narayanan, and J. Wang
UPD, Argonne National Laboratory, Argonne, Illinois 60439

Y. Yue and R. Cuenca
ESD, Argonne National Laboratory, Argonne, Illinois 60439

(Presented on 23 August 2001)

Intense x-ray sources coupled with efficient, high-speed x-ray imagers are opening new possibilities of high-speed time resolved experiments. The silicon pixel array detector (PAD) is an extremely flexible technology which is currently being developed as a fast imager. We describe the architecture of the Cornell PAD, which is capable of operating with submicrosecond frame times. This 100 $\times$92 pixel prototype PAD consists of a pixelated silicon diode layer, for direct conversion of the x rays to charge carriers, and a corresponding pixellated complementary metal–oxide–semiconductor electronics layer, for processing and storage of the generated charge. Each pixel diode is solder bump bonded to its own pixel electronics consisting of a charge integration amplifier, an array of eight storage capacitors and an output amplifier. This architecture allows eight complete frames to be stored in rapid succession, with a minimum integration time of 150 ns per frame and an interframe deadtime of 600 ns. We describe the application of the PAD to capture an x-radiograph movie of the mass-density distribution of the spray plume from internal combustion engine fuel injectors. [DOI: 10.1063/1.1435816]

I. INTRODUCTION

Intense x-ray sources coupled with efficient, high-speed area x-ray detectors are opening new regimes of high-speed x-ray imaging. Experiments of interest include contracting muscle, enzyme–substrate interactions, polymerization, materials failure, elastic deformation under stress, and field-induced changes in liquid crystals.[1–4] Modern synchrotron sources are sufficiently intense that the time resolution of many of these experiments are limited by the readout rates of available detectors, and not by the number of x rays. Although detectors based on large-format charge coupled devices (CCDs) have improved the situation somewhat, CCD detectors are generally limited to successive frame rates of roughly a millisecond. There is a pressing need for large-format, large area detectors which can frame at microsecond, or even faster rates. Here, we describe a pixel array detector (PAD) technology that is suited to this challenge.

II. PIXEL ARRAY DETECTOR ELECTRONICS

The PAD we have constructed is a two-layer device consisting of a 300-μm-thick high-resistivity silicon diode array layer flip chip bonded to a pixellated complementary metal–oxide–semiconductor (CMOS) layer. X rays are stopped in the diodes and result in the creation of electron–hole pairs. This charge is then processed by the underlying CMOS layer. The detector is fully parallel in that each diode has its own signal processing and storage electronics on the CMOS layer. The true flexibility of the PAD architecture becomes apparent when one considers what is necessary to modify the functionality of the detector. The PAD presently in use at Cornell University is an analog current-integrating detector. However, once the infrastructure of flip-chip bonding is in place, dramatically different detector designs tailored to specific applications may be implemented simply by changing the electronics integrated into CMOS layer. So, for example, other groups working on x-ray PADs for more count-rate forgiving applications have chosen to implement digital designs in which the photons are individually counted.

The Cornell PAD detector is designed to acquire up to eight successive frames of data with submicrosecond time resolution. After all eight frames of data have been acquired, the signal from the diode layer is electronically gated off and the stored data is read out at relatively slow rates. Each pixel contains an integrating input amplifier, an array of eight storage capacitors, and an output amplifier (Fig. 1). The pixel architecture and testing of a small (4×4 pixel) version of this device has been described.[5–7] More recently, a larger 100×92 pixel version was evaluated.[8]

Several new pixel structures are now in test stages of development at Cornell University. For example, we are designing a ''push–pull'' structure which is designed so that charge is alternately integrated on one capacitor while the

[a]Electronic mail: renzi@bigbro.biophys.cornell.edu
[b]Also at: CHESS, Cornell University, Ithaca, New York 14853.

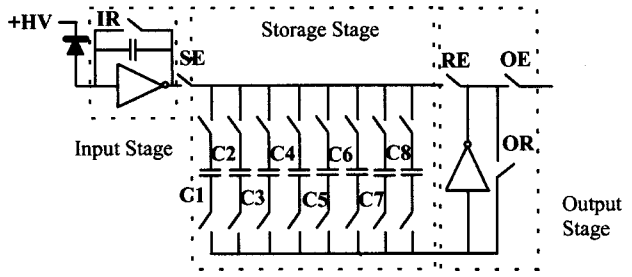

FIG. 1. Electronics integrated into each pixel of the PAD. Charge produced by the conversion of x rays within the diode is integrated onto the capacitor in the input stage. Rapid imaging is accomplished by storing the integrated voltage of successive images onto one of eight storage capacitors (C1–C8). Digital switching logic is used to select the desired capacitor. On readout, each capacitor is connected in succession to the output amplifier which is multiplexed to a buffer amplifier at the end of each pixel row. Also shown are various pixel control switches: IR, integrator reset; SE, store enable; RE, read enable; OE, output enable; and OR, output reset.

other is being read out, so that framing may proceed indefinitely without readout pauses. The limitation to this design is the speed at which the entire detector can be read out, which is mainly limited by the number of analog-to-digital output channels on the detector. This detector is designed with the capability of being switched into a five capacitor rapid-storage mode, similar to the present device.[8] In practice, we envision this PAD as being operated in a video-rate-like push–pull mode for sample alignment and survey work, with the capability of acquiring rapid, successive frames of particularly interesting parts of the data.

III. PAD DESIGN CONSIDERATIONS

A typical PAD user would like a detector with large area (many cm across), large format (e.g., $>1000\times1000$ pixels), minimal dead area, and high radiation tolerance. The large area and large format are not feasible with a single silicon die, necessitating detectors consisting of several dies to tile a larger area. For example, the 92×100 pixel PAD prototype was fabricated with a (now obsolete) Hewlett–Packard (HP) 1.2 μm process. This process had several limitations: First, the process was not radiation hardened, so the CMOS layer would start to die after relatively modest x-ray exposure. Second, the relatively large features of a 1.2 μm necessitated a large pixel 150 μm across. Third, the process allowed a maximum die size of only 15 mm$\times$15 mm. The trends within the semiconductor industry towards smaller processes have worked very much in favor of the PAD designer. So, for example, our newest design has been fabricated with a 0.25 μm Taiwan Semiconductor Manufacturing Corp. (TSMC) process with a maximum die size of 21.5 mm$\times$21.5 mm. This has allowed a large format array (209×213 pixels) of smaller pixels (100 μm across) with greater functionality and (see below) greater radiation hardness.

IV. RADIATION TOLERANCE

A typical problem for CMOS electronics exposed to x rays is long term damage to the oxide layer of the *n*-type metal–oxide–semiconductor (NMOS). The mobilities of electrons and holes, created by x rays stopped in the oxide differ by many orders of magnitude. Although the electrons are generally able to leak out, the holes become trapped and positively charge the oxide. This positive space charge between the field-effect transistor (FET) gates and channels leads to a monotonic drift of the transistor threshold voltages. Another important radiation-damage effect is increased leakage of the transistors.

As an illustration, the 92×100 PAD showed significant damage after 300 krad dose (referred to the SiO_2). The PAD is adversely effected by both the increase in leakage current and the change in threshold value. Due to the analog construction of the amplifiers, shifts in threshold and leakage current lead to shifts in the background value. The total well depth of the pixel depends upon the dc background value, i.e., when the background shifts the total voltage available for integration shifts. In the case of the PAD, this means that the pixel continues to function, but eventually the damage compromises the well depth. A sample of the damage on the 92×100 PAD after 300 krad (SiO_2) is shown in Fig. 2.

Two methodologies are being used at Cornell to raise the radiation damage threshold. The first technique is simply to move to a smaller size process to avoid charging of the oxide. Smaller CMOS processes naturally use thinner oxide layers. It has been shown that the leakage rate of trapped holes in the oxide increases dramatically as the oxide thickness falls below about 20 nm.[9] Whereas the HP 1.2 μm process uses oxide layers 20.6 nm thick, the oxide layer in the 0.25 um TSMC process is only 5.7 nm thick. The second technique, which has been tested at CERN to deal with radiation-induced parasitic leakage, involves developing an enclosed layout transistor (ELT) in which the transistor source is completely surrounded by the gate, thereby minimizing leakage paths.[10] The physical layout of an ELT amplifier designed at Cornell for the PAD is shown in Fig. 3. CERN has demonstrated that the combination of a small process and ELT design raises the radiation damage threshold from about 30 krad to above 30 Mrad. Since these doses refer to absorption in the oxide, which is already shielded by the diode layer, the radiation hardness is raised to at least several hundred Mrad (referred to the detector face) at 10 keV, which is an acceptably long detector life for most applications. The current test amplifiers at Cornell show no damage at 3 Mrad to the oxide, with higher dosage testing to follow.

V. FUEL SPRAY RADIOGRAPHY

The benefits of a rapid-framing PAD are clearly seen in a fuel-injector spray radiography experiments performed at both the Advanced Photon Source (APS) and Cornell High Energy Synchrotron Source (CHESS). An understanding of the details of the atomization of the fuel is of great importance towards increasing the efficiency of an engine and towards reducing pollutants. The efficiency of the injector can be evaluated by studying the critical first few hundred microseconds of the injection process. Optical methods, which have typically been used in the past, are unable to reveal the true fuel mass distribution because the dense mixture of fuel droplets in air scatters light too strongly. However, the fuel

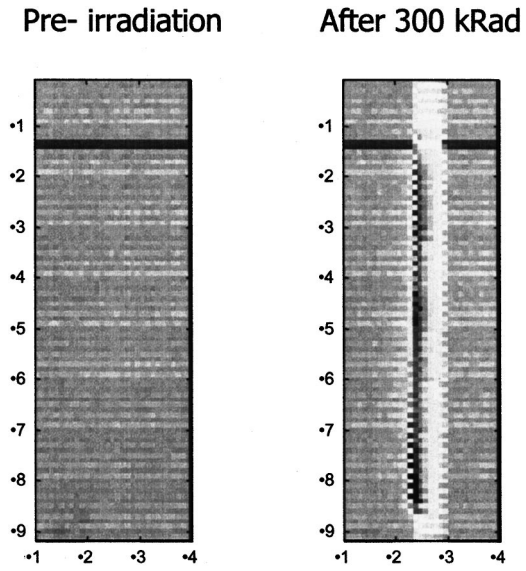

FIG. 2. Radiation damage to a 30×92 slice of a 92×100 PAD used in a radiography experiment. The darker gray level is the standard background. The white section represents an approximately 20% downwards shift in the background pedestal. In order to test for radiation damage, the direct synchrotron beam was allowed to fall onto the detector in a footprint outlined by the white area.

spray can be x-radiographed to directly reveal the mass density distribution, provided that the x-ray images can be acquired on the appropriate times scale steps of tens of microseconds.

Previous work on fuel spray radiography consisted of detecting the spray absorption with a point-detecting gated avalanche photodiode. This allowed fast acquisition of individual data points, but was a very slow method for mapping out the full spray behavior over an area. The point detection method did establish, however, that the fuel spray process had significant, and very reproducible, structural detail. In order to practically analyze the feasibility of different nozzle designs, it was necessary to acquire image radiographs of the entire spray.

The APS experiment consisted of studying the dynamics of an automobile fuel injector in 6.4 μs slices. A fuel-injector chamber with x-ray transparent windows was installed on beamline 1-BM at the APS. In order to increase x-ray contrast, the injection fluid was doped with a cerium additive and the radiographs were taken with an x-ray energy near the Ce absorption edge. The entire fuel spray was mapped out temporally for a total of 1.5 ms by taking multiple sets of time-shifted data. Because the footprint of the x-ray beam was considerably smaller than the 40 mm×25 mm area of the spray, it was necessary to build up a radiograph "movie" of the spray by acquiring successive time-slice images of the successive spray cycles at different positions of the spray relative to x-ray beam and detector. Repeated images of different fuel injections showed that the structural details of the spray were very reproducible at any given position and time after injection. A sample composite image from a gasoline fuel injector nozzle is shown in Fig. 4. Follow-up experiments at beamline D-1 at CHESS confirmed the injector behavior. Both gasoline and diesel (not shown) fuel injectors were studied.

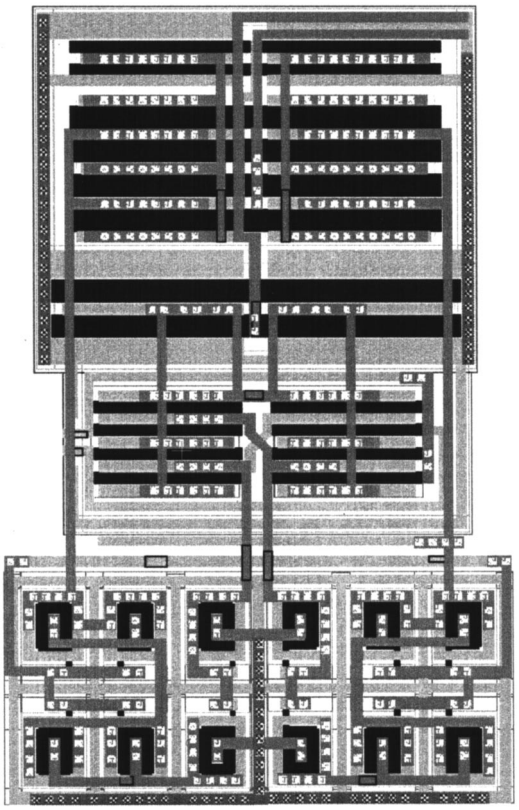

FIG. 3. Operational amplifier for both the integration and readout stages of the eight-capacitor structure. The *p*-type metal–oxide–semiconductor elements are designed as linear transistors; the NMOS elements are designed as ELT. The amplifier has been tested and performs with equivalent gain/noise to a linear counterpart.

Numerous unexpected structural details are visible in the radiographs. These details vary with the variables of the injector, such as the size, shape, and finish of the injector orifice, and are expected to have significant practical implications for the design of improved fuel injectors. Detailed results of these experiments will be published elsewhere.

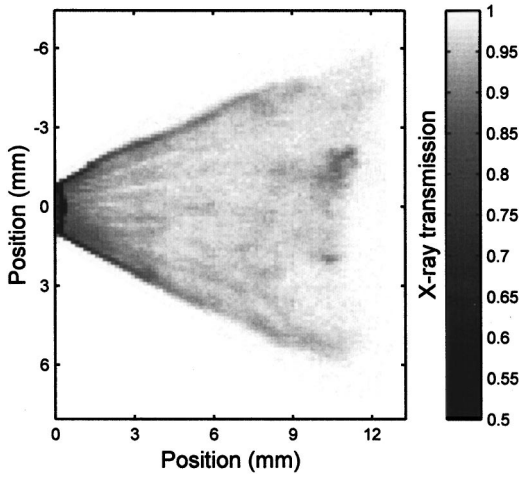

FIG. 4. Composite image of gasoline spray coming from a fuel injector. This is a 5 μs exposure taken 260 μs after the start of injection. The injector nozzle is positioned just below the (0, 0) mm point.

VI. CONCLUSION

PADs are a flexible technology which has already shown great utility in challenging fuel spray radiography experiments. These experiments have demonstrated that even well-known technologies may benefit from fast time-resolved x-ray probes. It is safe to predict that the availability of fast quantitative imagers will find a variety of uses in science and technology and extend the applications being performed at synchrotron radiation sources. Our goal is to continue to develop PADs and to make them available to the community for diverse time-resolved x-ray experiments.

ACKNOWLEDGMENTS

The authors would like to thank Martin Novak for his help in setting up these experiments. This work was supported by DOE Grant Nos. DE-FG-0297ER14805 and DE-FG-0297ER62443 and CHESS, which is a national NSF-supported facility under Grant No. NSF-DMR 97-13424.

[1] S. M. Gruner, Science **238**, 305 (1987).
[2] K. Moffat, Annu. Rev. Biophys. Biophys. Chem. **18**, 309 (1989).
[3] K. Moffat, Acta Crystallogr., Sect. A: Found. Crystallogr. **A54**, 833 (1998).
[4] W. Folkhard, E. Mosler, E. Geercken, E. Knorzer, H. Nemetschek-Gansler, and T. Nemetschek, Int. J. Biol. Macromol. **9**, 169 (1987).
[5] S. L. Barna, J. A. Shepherd, R. L. Wixted, M. W. Tate, B. G. Rodricks, and S. M. Gruner, Proc. SPIE **2521**, 301 (1995).
[6] S. L. Barna, J. A. Shepherd, M. W. Tate, R. L. Wixted, E. F. Eikenberry, and S. M. Gruner, IEEE Trans. Nucl. Sci. **44**, 950 (1997).
[7] E. F. Eikenberry, S. L. Barna, M. W. Tate, G. Rossi, R. L. Wixted, P. J. Sellin, and S. M. Gruner, J. Synchrotron Radiat. **5**, 252 (1998).
[8] G. Rossi, M. Renzi, E. F. Eikenberry, M. W. Tate, D. H. Bilderback, E. Fontes, R. Wixted, S. Barna, and S. M. Gruner, J. Synchrotron Radiat. **6**, 1096 (1999).
[9] N. S. Saks, M. G. Ancona, and J. A. Modolo, IEEE Trans. Nucl. Sci. **31**, 1249 (1984).
[10] M. Campbell, G. Anelli, M. Burns, E. Cantatore, L. Casagrande, M. Delmastro, R. Dinapoli, F. Faccio, E. Heijne, P. Jarron, M. Luptak, A. Marchioro, P. Martinengo, D. Minervini, M. Morel, E. Pernigotti, I. Ropotar, W. Snoeys, and K. Wyllie, IEEE Trans. Nucl. Sci. **46**, 156 (1999).